The Development of an Intelligent Hybrid Active-passive Vibration Isolator

2016 J. Phys.: Conf. Ser. 744 012160

(http://iopscience.iop.org/1742-6596/744/1/012160)

The Development of an Intelligent Hybrid Active-passive Vibration Isolator

Changgeng Shuai [1,2,4], Jianguo Ma [1,2,5] and Emiliano Rustighi[3,6]

[1] Institute of Noise&Vibration, Naval University of Engineering, Wuhan 430033, P.R.China
[2] National Key Laboratory on Ship Vibration&Noise, Wuhan 430033, P.R.China
[3] Institute of Sound and Vibration Research, University of Southampton, UK

Email: [4] chgshuai@163.com, [5] mjianguo0722@163.com, [6] er@isvr.soton.ac.uk

Abstract: A hybrid active-passive vibration isolator made up of electromagnetic actuator and air spring in parallel can be used to effectively isolate the broadband and line spectrum vibration of mechanical equipment simultaneously. However, due to its reliability and safety problems caused by the impact, its application in ships is limited. In this paper, an impact-resistant structure and an air gap self-sensing method of the passive-active hybrid vibration isolator are proposed and developed on the base of modelling, simulation and analysis. A thin magnetic rubber is filled into the air gap of electromagnetic actuator, which can avoid rigid collision between the armature and the permanent magnet under the action of impact. A suspension armature structure including pre-compression spring is suggested, which can automatically compensate the deformation caused by impact and protect the coil and permanent magnet from impact damage. An air gap self-sensing method is developed through detecting the voltage between the input and output terminals of actuator, which is verified by experiments.

1. Introduction

Vibration isolation is one of the most direct and effective way to control ship machinery noise. Passive vibration isolation technology has been applied for decades, and the best vibration isolation effect of arrives to 40-50dB in some engineering applications[1]. However, it cannot effectively isolate low frequency line spectrum vibration[2]. Many studies[1-2] showed that the passive-active hybrid vibration isolation mount composed of rubber isolator and piezoelectric, magnetostrictive or active inertial actuator can effectively control broadband and low frequency vibration simultaneously. However, they can hardly been widely applied in ship due to their shortcomings of limited bearing capacity, low impact-resistant reliability and poor adaptability to the onboard environment[3]. In recent years, Lin H.[4-6] proposed a new electromagnetic actuator-air spring hybrid vibration isolation system, in which the air spring mainly carried the weight of the power device and efficiently isolated its broadband vibration, and the electromagnetic actuator integrated into air spring in parallel was used to actively eliminate residual low frequency line spectrum vibration. The attitude of isolation system and the average air gap of actuator were monitored by the use of the eddy current displacement sensor. The reference signal and control target function in the system were achieved by the acceleration sensor. The results showed that the hybrid isolation system could effectively isolate the broadband and line spectrum vibration of mechanical equipment simultaneously. However, its application is limited

because of the lack of stability and safety for the hybrid vibration isolation system when ship swing or under transient impact[7-9]. Once the eddy current displacement sensor and the acceleration sensor fail, the system would not be able to recognize and control the attitude and vibration response of the system. Moreover, the existing displacement sensing technology can only acquire the average air gap of actuator, which is clearly not accurate for large-scale isolation systems.

To improve the reliability and security of passive-active hybrid vibration isolation system in marine applications, and simplify the system architecture, this paper proposes a design concept of impact-resistant displacement self-sensing intelligent passive-active hybrid vibration isolator and studies its basic principles and properties. This attempt will be of great significance for solving the onboard application challenges of passive-active hybrid vibration isolation technology.

2. Modeling and Simulation of Electromagnetic Actuator

2.1. Theoretical model and experimental verification

Figure 1 shows the permanent magnet biased electromagnetic actuator mainly including iron core, armature, coil and permanent magnet, in which the thickness of the permanent magnet is h_m, the air gap is z, the width of the left and right arms of the iron core all is a_1, and half the width of the intermediate iron core is a_2. The permanent magnet provides a biased force. When the coil inputs alternating current, the actuator will output the alternating activation force.

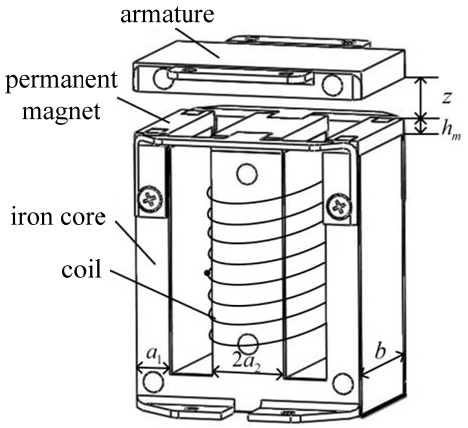

Figure 1. Schematic diagram of permanent magnet biased electromagnetic actuator.

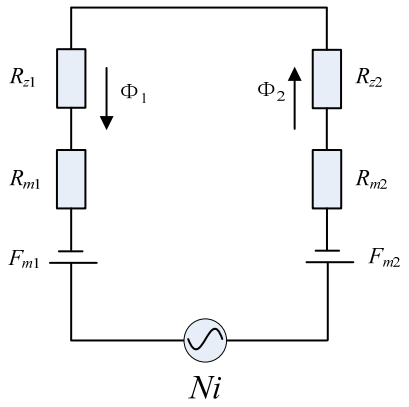

Figure 2. The equivalent magnetic circuit of U-shaped actuator.

To simplify the analysis, the magnetic flux leakage and the magnetic resistance of the iron core and armature in Figure 1 are ignored, and the iron core is split into two U-shaped core structures. The equivalent magnetic circuit of the U-shaped actuator is shown in Figure 2, in which N represents the coil turns; i is the control current; F_{m1} and F_{m2} represent the equivalent magnetic potential on both sides of the permanent magnet, respectively; R_{m1} and R_{m2} represent the equivalent reluctance of permanent magnet; R_{z1} and R_{z2} represent the magnetic resistance on both sides of the air gap, respectively; Φ_1 and Φ_2 represent the magnetic flux on both sides of the air gap, respectively. The relations among these parameters can be expressed as:

$$F_{m1} = F_{m2} = H_c h_m \tag{1}$$

$$R_{m1} = \frac{H_c h_m}{B_r a_1 b}, \qquad R_{m2} = \frac{H_c h_m}{B_r a_2 b} \tag{2}$$

$$R_{z1} = \frac{z}{\mu_o a_1 b}, \qquad R_{z2} = \frac{z}{\mu_o a_2 b} \tag{3}$$

$$\Phi_1 = \Phi_2 = \frac{F_{m1} + F_{m2} + Ni}{R_{m1} + R_{m2} + R_{z1} + R_{z2}} = \eta \frac{Ni + 2H_c h_m}{z + \mu_0 \frac{H_c}{B_r} h_m} \tag{4}$$

where, H_c is the coercive force of permanent magnet; B_r is the residual magnetism; μ_0 is the air permeability; $\eta = \mu_0 \frac{a_1 a_2 b}{(a_1 + a_2)}$.

The output attractive force F_E of the electromagnetic actuator shown in Figure 1 can be expressed as:

$$F_E = \frac{\Phi_1^{\ 2}}{\mu_0 a_1 b} + \frac{\Phi_2^{\ 2}}{\mu_0 a_2 b} = \eta \frac{(Ni + 2H_c h_m)^2}{(z + \mu_0 \frac{H_c}{B_r} h_m)^2} \tag{5}$$

If no the control current in coil, the equation (5) can be simplified as

$$F_P = \eta \frac{4H_c^2 h_m^2}{(z + \mu_0 \frac{H_c}{B_r} h_m)^2} \tag{6}$$

where F_p is the biased attractive force of permanent magnet.

If the control current i is input into the coil, the output attractive force is increased or decreased when the magnetic field generated by the current is in the same or opposite direction as the biased magnetic field. Therefore, the activation force F_g needed for active control may be obtained and expressed as

$$F_g = F_E - F_P = \eta \frac{4H_c h_m Ni + N^2 i^2}{(z + h_m)^2} \tag{7}$$

where $H_c h_m$ is only related to the permanent magnet and can be large enough to satisfy $|4H_c h_m Ni| >> N^2 i^2$ through material selection and structural design. In this case, F_g can be approximated as

$$F_g \approx \eta \frac{4H_c h_m Ni}{(z + h_m)^2} \tag{8}$$

Equation (8) shows that the output electromagnetic activation force is approximately linear with the input control current of the actuator.

Figure 3 shows the theoretical and experimental results, in which the theoretical value of the output attractive force according equation (5) is greater than the experimental value because of ignoring the leakage flux and magnetic reluctance of the iron core in the theoretical model.

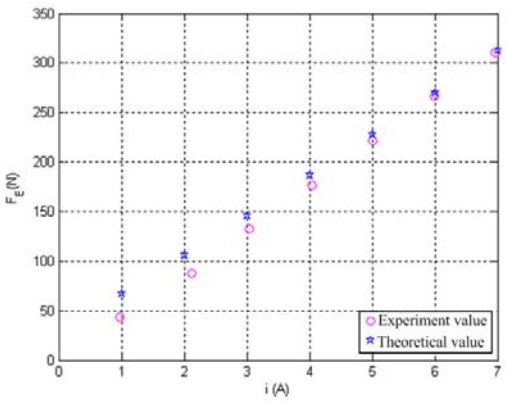

Figure 3. Theoretical and experiment results of the output attractive force F_E.

2.2 Simulation and Experiment

A three-dimensional actuator model is built in ANSYS, as shown in Figure 4. In the model, the leakage flux of air gap and the non-linearity of different permeability magnetic materials are considered. Given the boundary conditions, the magnetic density distribution and the vector of magnetic field lines can be obtained accurately, as shown in Figure 5. The electromagnetic activation forces of the actuator under different currents can thus be calculated accurately, as shown in Figure 6, which is consistent with the experimental results.

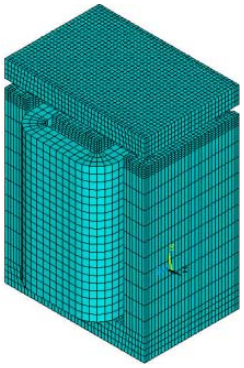

Figure 4. Finite element model of the electromagnetic actuator.

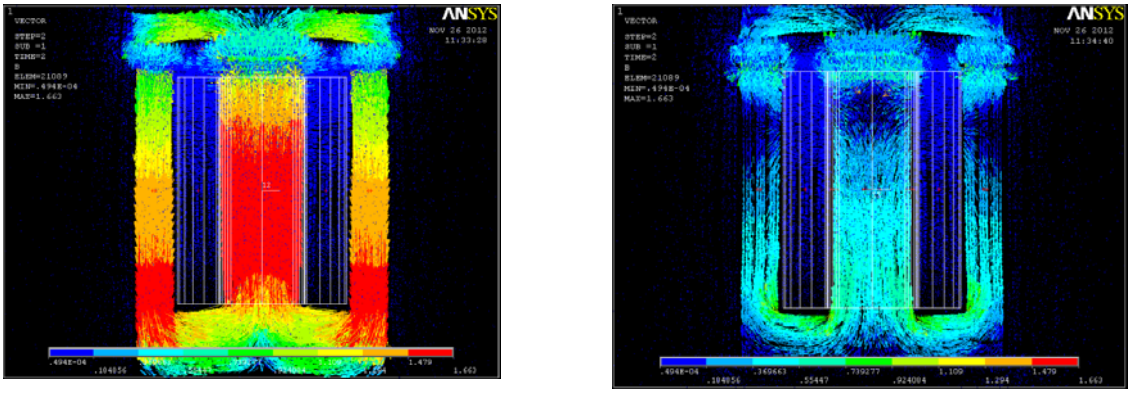

(a) The directions of electromagnetic and permanent magnetic field are identical

(b) The directions of electromagnetic and permanent magnetic field are opposite

Figure 5. Vector plot of magnetic flux of the electromagnetic actuator with input control current.

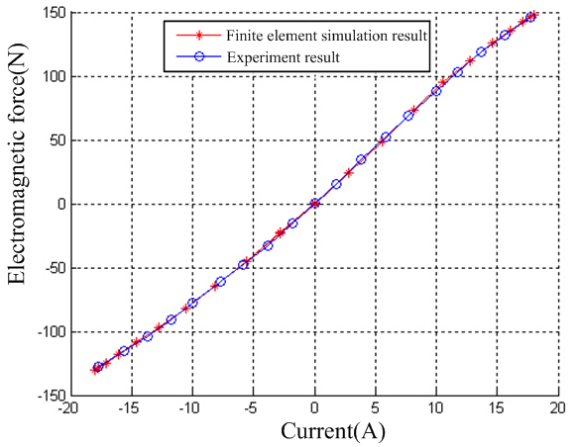

Figure 6. Simulation and experiment results of electromagnetic activation force.

3. Stability and Impact-resistant Design of Passive-active Hybrid Vibration Isolator

According to equation (5), the stiffness k_p of actuator can be expressed as

$$k_p = \frac{\mathrm{d}F_E}{\mathrm{d}z} = -2\eta \frac{(Ni + 2H_c h_m)^2}{(z + \mu_0 \frac{H_c}{B_r} h_m)^3} \tag{9}$$

which is always negative and is inversely proportional to the cube of air gap z. Figure 7 shows the relation of the stiffness of air spring, electromagnetic actuator and their hybrid vibration isolator to the air gap z. From the figure, when z decreases to a certain extent, the stiffness of the passive-active hybrid vibration isolator will be lessen than zero, that is, the output attractive force of actuator is greater than the support force of air spring. In this case, the hybrid vibration isolation system may lose its balance.

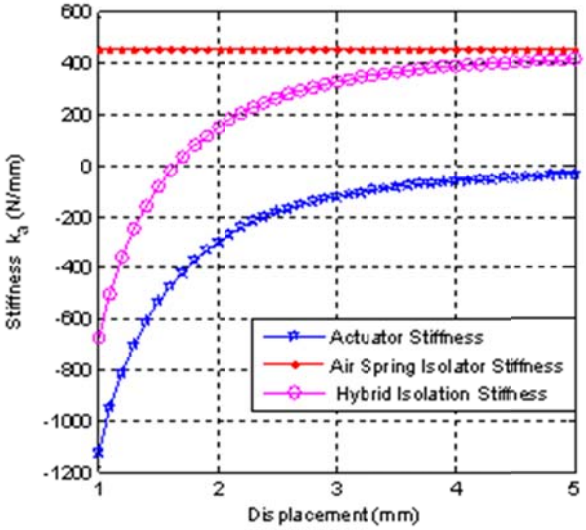

Figure 7. Stiffness variation curves of air spring, electromagnetic actuator and their hybrid vibration isolator with the air gap z.

In addition, the passive-active hybrid vibration isolator used in ships may fail by the rigid collision between the permanent magnet and the armature due to the large deformation under impact, swing, tilting and other stimulating effects.

In this paper, two solutions are proposed to solve the above problems of the instability and impact protection for the passive-active hybrid vibration isolator. First, the air gap between the armature and the permanent magnet is filled with a magnetic rubber to increase the magnetic permeability and the output power of the actuator, and avoid the rigid collision between the armature and the permanent magnet due to the large deformation at the same time. Second, a suspension armature structure composed of pre-compression spring is suggested, which can automatically compensate the deformation caused by impact and protect the permanent magnet from rigid contact with the armature. The structure of the impact-resistant passive-active hybrid vibration isolator is shown in Figure 8.

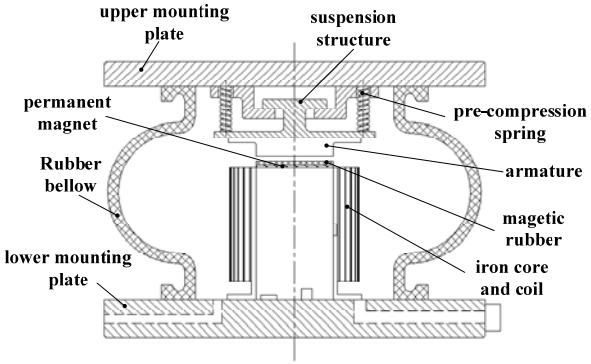

Figure 8. The structure of passive-active hybrid vibration isolator.

The simplified kinetic models of the vibration isolator before and after the contact of the armature with the magnetic rubber are shown in Figure 9. In the figure, k_a is the air spring stiffness, k_r is the magnetic rubber stiffness, and k_s is the pre-compression spring stiffness. They satisfy $-k_p<<k_s<<k_r$. The stiffness of the hybrid vibration isolator before and after contact can be expressed as follows:

Before contact,

$$k = k_a + k_p \tag{10}$$

After contact,

$$k = k_a + \frac{(k_p + k_r)k_s}{k_p + k_r + k_s} \approx k_a + k_s \tag{11}$$

(a) Before contact (b) After contact

Figure 9. Dynamic models of the hybrid vibration isolator before and after contact of the armature with the magnetic rubber.

According to equation (10), the stiffness k of the passive-active hybrid vibration isolator may be less than zero when the air gap z decreases to a certain extent as shown in Figure 8. In this case, the attractive force of electromagnetic actuator is greater than the support force of air spring and pulls the armature to the permanent magnet. This means that the hybrid vibration isolation system will lose its balance. In order to realize the stability of passive-active hybrid vibration isolation system, the hybrid isolator stiffness should always satisfy $k> 0$. From equation (9), (10) and (11), assuming the air gap z unchanged, the proper design of magnetic rubber filled in the air gap can make the hybrid isolator stiffness always greater than zero and assure the system stable operation before and after contact of the armature with the magnetic rubber. In addition, the filled magnetic rubber can increase the magnetic permeability and the output power of the actuator, and avoid the rigid collision between the armature and the permanent magnet due to the large deformation.

Suppose

$$z=x_0+h_r \tag{12}$$

where, h_r is the magnetic rubber thickness; x_0 is the actual air gap between the armature and magnetic rubber.

With equation (9), (10) and (12), the thickness of filled magnetic rubber must meet

$$\left(\frac{2\eta}{k_a}(Ni+2H_c h_m)^2\right)^{\frac{1}{3}} - \mu_0 \frac{H_c}{B_r} h_m < h_r < z - x_0 \tag{13}$$

In this case, the vertical stability of the passive-active hybrid vibration isolation system will be ensured.

A hybrid vibration isolator had been designed and produced. Its main parameters can be demonstrated as: the air gap z = 5mm, the thickness of magnetic rubber h_r=3mm. A vertical static load test is conducted to the hybrid vibration isolator and the experimental result is shown in Figure 10. From the figure, the static stiffness of the hybrid vibration isolator is small and always positive when the vertical displacement is less than 2mm, and the hybrid vibration isolator is always stable. When the displacement increases to more than 2mm, the armature will be in contact with the magnetic rubber. Then, the magnetic rubber will be deformed under load while the suspension armature structure does not work. The stiffness of hybrid vibration isolator will increase sharply. As the deformation continues, the pre-compression spring in the suspension armature structure will be compressed and the stiffness of hybrid vibration isolator quickly decreases, which will protect the actuator against the damage. When the load is relaxed, the system can be recovered automatically.

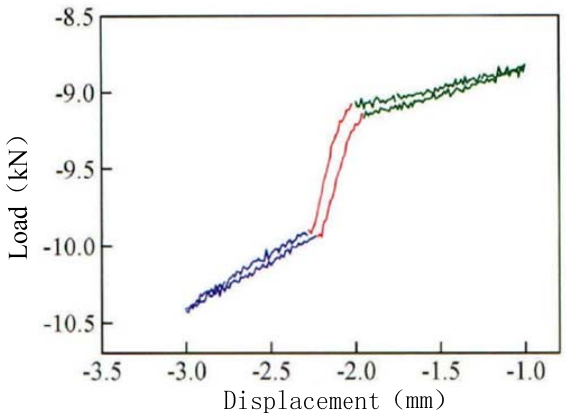

Figure 10. Vertical static load-deformation curve of the hybrid vibration isolator.

4. Self-sensing Air Gap in Actuator

4.1 Principle of self-sensing air gap

Based on the sensorless electromagnetic bearing principle[10-13], the coil inductance of the electromagnetic actuator can be expressed as

$$L_E = \frac{2\eta N}{z + h_m} \tag{14}$$

Figure 11 shows the relation of the inductance L_E to the air gap z according to the equation (14). From the figure, the coil inductance decreases as the air gap increases.

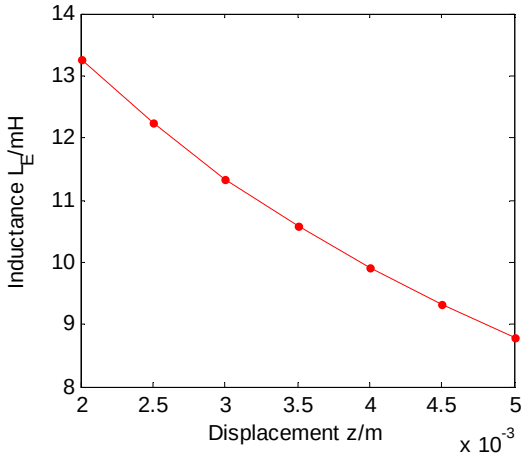

Figure 11. Variation curve of the inductance L_E with the air gap z.

Supposing the control current input into the actuator coil is $i=I_0\cos\omega_0 t$, the voltage on both ends of the coil would be

$$u_1(t) = (\mathrm{j}\omega_0 L_E + R_E)i \tag{15}$$

Where, R_E is the resistance of the actuator coil.

Ignoring the voltage drop caused by the coil resistance, substituting equation (15) into Equation (14), it can be obtained as

$$u_2(t) = (\mathrm{j}\omega_0 \frac{2\eta N}{z+h_m} + R_E) I_0 \cos\omega_0 t \tag{16}$$

Since R_E is a small amount, the voltage in the coil resistance can be ignored, then demodulating, multiplied by the cosine of the unit:

$$\begin{aligned} u_3(t) &= \mathrm{j}\omega_0 \frac{2\eta N}{z+h_m}\cos^2\omega_0 t \\ &= \mathrm{j}\omega_0 I_0 \frac{\eta N}{z+h_m}(1+\cos 2\omega_0 t) \end{aligned} \tag{17}$$

Through the low-pass filter, removing the component of 2 times the center frequency, the armature voltage signal can be obtained that:

$$u_4(t) = \mathrm{j}\omega_0 \eta N I_0 \frac{1}{z+h_m} \tag{18}$$

Let $z = z_0 + z_x$, where z_0 is the initial gap and z_x is the vertical deformation. Expanding equation (18) as the Taylor series at the initial gap z_0 and neglecting the higher-order terms, equation (19) can be simplified as

$$u(t) = \frac{\mathrm{j}\omega_0 \eta N I_0}{z_0+h_m}\left(1-\frac{z_x}{z_0+h_m}\right) \tag{19}$$

From the equation (19), the voltage on both ends of the coil is proportional to the vertical deformation z_x. Based on this, the dynamic air gap can be calculated by measuring the voltage.

4.2 Experiment on self-sensing air gap

An experiment on self-sensing the air gap is conducted on an electromagnetic actuator with the output activation force of 300N as shown in Figure 12. In the figure, the armature and iron core of electromagnetic actuator are fixed under an upper steel plate and on a base steel plate respectively. The air gap between the armature and the iron core can be changed by replacing the gasket under the base steel plate. A differential voltmeter is used to measure the voltage on both ends of the coil. The main parameters of the actuator are: $a_1=a_2=2\times10^{-2}$m; $b=7.8\times10^{-2}$m; $h_m=4\times10^{-3}$m; N = 200; $B_r=1.27$; $H_c=9.88\times10^5$; $I_0=1$A;$\omega_0=160\ \pi$ Hz . The amplitude of fundamental frequency of theoretical and testing voltage is obtained by Fourier transform. The variational values with the air gap are plotted in Figure 13. It can be found that the actual voltage is almost linear with the air gap, and the theoretical and experimental results are consistent.

Figure 12. Test rig of self-sensing the air gap.

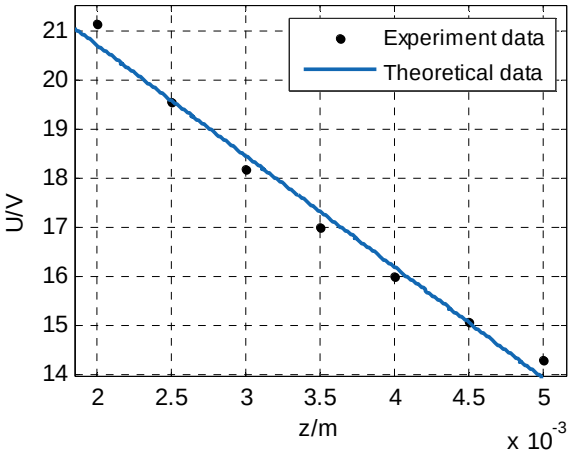

Figure 13. Voltage variations with the air gap in theory and experiment.

5. Conclusions

In this paper, an impact-resistant intelligent passive-active hybrid vibration isolator is proposed and developed to solve the on-board application challenges of the passive-active hybrid vibration isolation technology. The following conclusions can be drawn.

(1) The theoretical attractive force of electromagnetic actuator on the base of the equivalent magnetic circuit model is larger than the experimental value due to ignoring the leakage magnetic flux and the magnetic reluctance of the iron core. The simulated electromagnetic activation forces of the actuator based on the magnetic field analysis by finite element is consistent with the experimental results.

(2) The proper design of magnetic rubber filled into the air gap can avoid the rigid collision between the armature and the permanent magnet due to the large deformation and ensure the stability

of the passive-active hybrid vibration isolation simultaneously. The suspension armature structure including pre-compression spring can automatically compensate the deformation caused by impact and protect the coil and permanent magnet from being destroyed. Theoretical and experimental results show that the developed impact-resistant hybrid vibration isolator is feasible.

(3) The voltage between the input and output terminals of actuator is approximately linear with the air gap. Based on this, an air gap self-sensing method is proposed and developed. The theoretical and experimental results are consistent.

Acknowledgement
This work was funded by China Scholarship Council (CSC), and supported by Program for New Century Excellent Talents in University (NCET) from Chinese Ministry of Education and the National Natural Science Foundation of China within Grant No. 51303209. The supports are greatly appreciated. The authors would like to acknowledge the support of Institute of Sound and Vibration Research, University of Southampton, UK.

References

[1] Lin H 2007 Development of Submarine Acoustic Stealth Technology *Ship Science and Technology* **9**(5) 29-42
[2] Lin H, and Wei X 2013 Ship Vibration Isolation Technology and Its Progress *Acta Acustica* **38**(2) 128-136
[3] Yan L, Lin H and Changgeng S. 2015 Technical Study of Maglev Suspension - Air Spring Vibration Isolation Mounts for Marine Machinery *Acta Acustica* **40**(5) 751-760
[4] Lin H and Yan L 2013 Theory and Experiment of Passive-Active Hybrid Vibration Isolation Mounts Using Electromagnetic Actuator and Air Spring *Acta Acustica* **38**(2) 241-249
[5] Lin H, Yan L and Changgeng S 2015 Active-Passive Vibration Isolation for Ship Machinery Using Electromagnetic Actuator and Air Spring *The 22st International Congress on Sound and Vibration*. 12-16 July, Florence/Italy
[6] Yan L, Lin H and Changgeng S 2015 Multi-channel Narrow-band Fx-Newton Time Frequency Algorithm and Dynamic Mechanical Active Vibration Isolation Experiment *Acta Acustica* **40**(3) 391-403
[7] Wangsheng Q and Hua Z 1996 Development Impact-resistant Vibration Isolator *Mechanical and Electrical Equipment* **4** 36-40
[8] Yuhong X, Hongyuan J and Haodong W 2009 Shock Protection Characteristics of Metal Rubber Isolators *Journal of Vibration and Shock* **28**(1) 72-75
[9] Cheng Z 2012 *Theoretical Modeling and Experimental Analysis of Non-Linear Shock Characteristics of Rubber Isolator* PHD dissertation, Shanghai: Shanghai Jiaotong University
[10] Jun W 2005 *Study on Self-sensing Active Magnetic Bearing* PHD dissertation. Nanjing: Nanjing University of Aeronautics and Astronautics
[11] Mizuno T and Boeuler H 1995 Self-sensing magnetic bearing control system design using the geometric approach *Control Engineering Practice* **3**(7) 925-932
[12] Mizuno T, Ishii T and Araki K 1998 Self-sensing magnetic suspension using hysteresis amplifiers *Control Engineering Practice* **6**(9) 1133-40
[13] Noh M D and Malsen E H 1997 Self-sensing magnetic bearings using parameter estimation *IEEE Transactions on Instrumentation and Measurement* **46**(1) 45-50